

Accuracy of Trajectory Calculation in a Finite-Difference Circulation Model*

JOHN R. BENNETT [†] AND ANNE HUTCHINSON CLITES

*U.S. Department of Commerce, Great Lakes Environmental Research Laboratory,
2300 Washtenaw Avenue, Ann Arbor, Michigan 48104*

Received March 25, 1985; revised March 25, 1986

The prediction of drifting object motion due to currents in an irregular body is a complex problem with a wide range of practical applications. Simple numerical methods for interpolating current velocity fields have spatial interpolation and time integration errors that result in misleading solutions. The method described in this paper minimizes these problems, yielding much more accurate predictions. This method can be easily implemented in other finite-difference models or finite-element models. © 1987 Academic Press, Inc.

INTRODUCTION

An important practical application of lake and ocean circulation models is the prediction of drifting object trajectories for search and rescue operations or oil and chemical spill cleanup. This type of forecasting involves four basic steps. First, wind stress is determined from either predicted or observed winds and the air-water temperature difference. Second, currents are calculated from the wind stress, the initial and boundary conditions, and the density field. Third, currents and winds are used to compute trajectories. Finally, when forecasting the movement of oil or chemicals, the effects of physical or chemical transformations must be estimated. This paper will examine errors introduced in the third of these four steps, the computation of trajectories in a closed basin and the methods developed here to avoid those errors.

The numerical method described in this paper is used to calculate the current-induced portion of the particle trajectories in lakes, but it would be very simple to implement in other finite-difference models or in finite-element models. It is far more accurate in time and space than simple first-order methods. The spatial interpolation of currents used in this second-order method allows particles to move along a jagged finite difference coast without running into the boundary and becoming artificially "beached" or trapped in grid corners.

There are several operational spill models available [1, 4-6]. Of necessity, com-

* GLERL Contribution No. 442.

[†] Current address: Environmental Research Institute of Michigan, P.O. Box 8618, Ann Arbor, Mich. 48107.

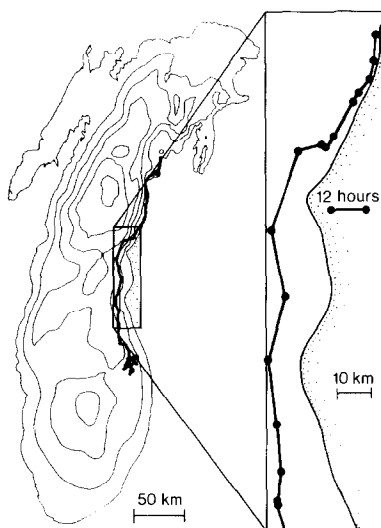


FIG. 1. Path of a satellite-tracked drifter in Lake Michigan from 15 September to 16 October 1982. The 50-m isobaths are marked. The inset shows an enlarged view of the drifter track following the coast. The positions are marked at 12 h intervals.

promises are made between physical or numerical accuracy and ease of operation. The intent of this study was to improve the numerical methods used in the Great Lakes spill model developed by Pickett [1] and modified by Schwab et al. [4]. This model is used by the National Weather Service and the Coast Guard to predict movement of oil or chemical spills to facilitate their containment and cleanup. In parallel to this theoretical work, satellite-tracked drifter buoys are being used to gather data for model verification [2]. Figure 1 shows a track of one of these drifters in Lake Michigan. The track follows the irregular shoreline quite closely for long periods. Moreover, some of the highest speeds are observed when the drifters are in the coastal current, often within 10 km of shore. This type of path is very difficult to model numerically. Earlier attempts have not been successful in keeping the particle trajectories from crossing the shoreline or from becoming trapped in the grid corners. The finite-difference method presented here minimizes these kinds of errors.

A METHOD FOR CALCULATING TRAJECTORIES

In this model, particle trajectories are calculated from a combination of current and wind using two assumptions:

- (1) When there is no wind, a particle cannot cross the shore boundary.
- (2) When particles are driven ashore by the wind, they stay there.

The reasoning behind these assumptions is that, in the absence of flooding, the currents are parallel to shore; thus, only wind can cause particles to beach. In practice, surface waves can also carry particles towards a beach, but, in the Great Lakes, these waves are strongly correlated with the wind. The exact magnitude of the wind-driven flow depends on the nature of the particle. For example, a life jacket would have a large wind exposure but a body would have a small one.

The equations that describe particle motion are

$$\frac{dx}{dt} = u(x, y, t) + au_a(x, y, t) \tag{1}$$

$$\frac{dy}{dt} = v(x, y, t) + av_a(x, y, t), \tag{2}$$

where dx/dt and dy/dt are the particle velocity components, u and v are the x and y components of the current, a is the wind factor (the ratio of the wind-driven particle speed to the wind speed), and u_a and v_a are the x - and y -components of the wind. The currents used here were calculated from an incompressible model [4, 7]. They are obtained by dividing the mass transport components, U and V of Fig. 2, by the water depth.

The variables are defined at the points shown in Fig. 2 of each grid box in the bathymetric grid. The x -component of transport is defined at the center of the right

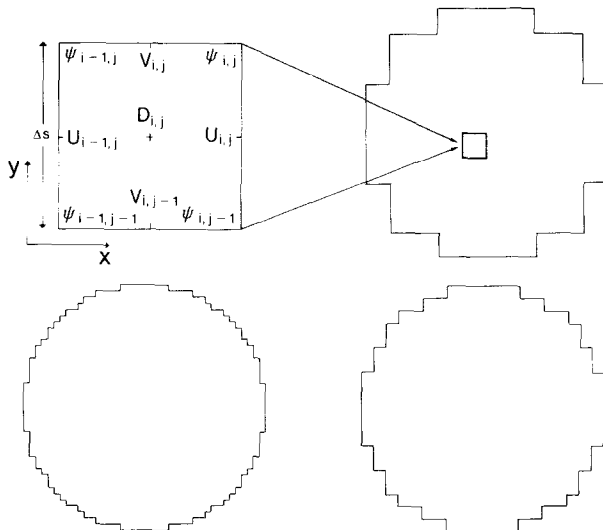


FIG. 2. Pictorial representation of the grid box and lake outlines for each of three grid sizes tested: 10, 5, and 2.5 km. Water depth (D) is defined at the center of the grid box, the x -component of transport (U) at the center of the sides, and the y -component of transport (V) at the center of the top. Stream-function (ψ) is defined at the corners.

side of the grid box and the y -component at the center of the top. Water depth is interpolated to the stream function points at the corners. To ensure that particles can be driven across the shore boundary only by wind, never by current alone, wind- and current-driven motion are calculated separately at each time step. For the operational lake trajectory model, the time step is chosen internally by the program to ensure that no particle can travel more than one-eighth the distance across a grid box in one time step. The value of one-eighth is arbitrary, but is small enough so that the trajectories do not significantly depend on the time step. The exact formulation of the time step for other applications would depend on the accuracy required and on other factors.

During the wind step, the following first-order difference equations govern particle motion:

$$x^{n+1} - x^n = \Delta t \cdot a \cdot u_a(x^n, y^n) \quad (3)$$

$$y^{n+1} - y^n = \Delta t \cdot a \cdot v_a(x^n, y^n). \quad (4)$$

This straightforward method is adequate since the wind has a simple spatial structure.

Predicting motion due to lake currents is more complex for several reasons. First, the simplest methods for interpolating the velocity field give rise to particle trajectories that either cross the shore boundary or trap particles that are near the boundary in the grid corners. Second, the (forward) Euler first-order derivatives have persistent errors that cause the particles to drift toward the boundary. The method developed in this paper for interpolating the velocity components minimizes the first problem, and a second-order time stepping procedure solves the second.

Spatially, the currents, defined numerically at the center of the sides of the grid boxes, are interpolated to the corners of the grid boxes (ψ in Fig. 2). This process is done carefully to ensure that the boundary values are extrapolated from the interior. Referring to Fig. 2, every corner point has north-south components of velocity on its right and left, and east-west components above and below it. Away from the shore boundary, interpolated values of the velocity components are formed by averaging these components. However, if one of these components is a zero shore value, the nearest interior value of that component is used instead. This prevents artificial "dead" zones from developing in the grid corners. This step may not be appropriate in a model that used a no-slip boundary condition. Once the velocity components are interpolated to the corners of all grid boxes, the new particle positions are predicted from

$$\frac{x^{n+1} - x^n}{\Delta t} = u(x^n, y^n) + \frac{1}{2} \frac{\partial u}{\partial x} (x^{n+1} - x^n) + \frac{1}{2} \frac{\partial u}{\partial y} (y^{n+1} - y^n) \quad (5)$$

$$\frac{y^{n+1} - y^n}{\Delta t} = v(x^n, y^n) + \frac{1}{2} \frac{\partial v}{\partial x} (x^{n+1} - x^n) + \frac{1}{2} \frac{\partial v}{\partial y} (y^{n+1} - y^n). \quad (6)$$

These formulas were derived from Taylor series expansion about the old particle position. The values of u , v , and their derivatives are computed by bilinear interpolation from the four corner points of the grid square in which the particle begins the time step. Once this has been done, the pair of simultaneous linear equations, (5) and (6), can be solved directly, yielding the new particle positions.

ACCURACY OF TRAJECTORY CALCULATIONS

The accuracy of trajectory calculations can be described by comparing them with trajectories resulting from solid rotation motion and wind-driven motion. This will be done here in three stages. First, the errors in the trajectories of particles in unbounded circular flows will be calculated. Second, the effects of shorelines on the trajectories will be evaluated numerically. Finally, calculated trajectories of particles in a complex, time-dependent wind-driven flow with various grid resolutions will be presented. The case of unbounded flow can be broken down further into solid rotation flow and rotational flow with variable vorticity. The solid rotation case is used to evaluate time differencing errors; the variable vorticity case is used to study the spatial interpolation errors.

The two velocity components in an unbounded solid rotation flow are

$$u = -\Omega \cdot y \quad (7)$$

$$v = +\Omega \cdot x, \quad (8)$$

where Ω is the angular rotation rate. Since these velocity components are linear functions of the spatial coordinates, bilinear interpolation on a finite-difference grid gives the exact solution for u , v , and their spatial derivatives. Thus, the accuracy will depend on the time step, Δt , but not on the grid size, Δs . Only two simple time differencing methods will be discussed here; the extension to other methods, however, is straightforward.

Using the complex representation of the position

$$Z = x + iy \quad (i = \sqrt{-1}) \quad (9)$$

the first- (forward Euler) and second-order (trapezoidal) methods are

$$\text{1st:} \quad \frac{Z^{n+1} - Z^n}{\Delta t} = i\Omega Z^n \quad (10)$$

$$\text{2nd:} \quad \frac{Z^{n+1} - Z^n}{\Delta t} = \frac{i\Omega}{2} (Z^{n+1} + Z^n). \quad (11)$$

The error, E , is defined as the difference between the starting position and the position one revolution later divided by the initial radius,

$$E = \frac{|Z^N - Z^0|}{|Z^0|}, \tag{12}$$

where $N = 2\pi/\Omega \Delta t$. N is the number of time steps required for the particle to complete the circle. Using the above formulas for the first- and second-order schemes yields

$$E_1 = |(1 + i\Omega \Delta t)^N - 1| \tag{13}$$

$$E_2 = \left| \left(\frac{1 + i\Omega \Delta t/2}{1 - i\Omega \Delta t/2} \right)^N - 1 \right|. \tag{14}$$

These formulas are plotted in Fig. 3. The maximum error for the second-order scheme, for $N < 2$, is about twice the radius. The reason for this is that, for the second-order scheme the radius is constant—the error is only in the phase. The farthest the particle can get from its initial position is on the opposite side of the circle. However, the first-order scheme gives an outward drift as well as a phase error; for small values of N (large time steps) the error can be nearly 14 radii (1400%). For the error to be less than one radius after one revolution using the first-order scheme requires about 30 time steps. The second-order scheme makes an error of less than 10% at about 15 time steps per revolution; clearly the slight increase in complexity is worthwhile.

As noted above, for solid rotation in an unbounded flow, the error does not depend on the spatial grid size. Thus, to evaluate the error as a function of Δt , one

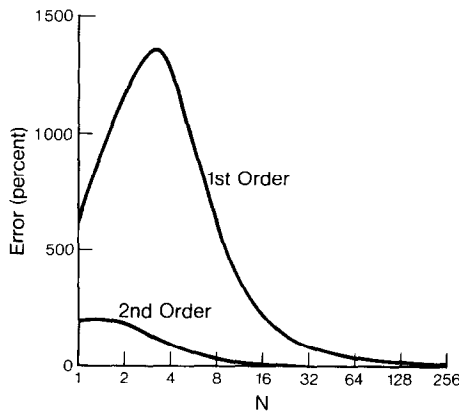


FIG. 3. Percentage error in the calculation of one revolution of a particle in a solid rotation flow for first- and second-order time difference schemes. Since, for solid rotation, there is no error in spatial interpolation of velocity, the error is only a function of N , the number of time steps per revolution.

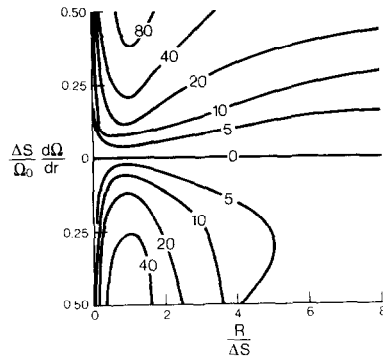


FIG. 4. Percentage error in the calculation of one revolution of a particle in a variable vorticity flow with perfect time differencing. The abscissa is the ratio of the initial radius R to the grid size. The ordinate is a measure of the percentage change in the vorticity per unit of grid size.

must consider a flow where the velocity components vary with the spatial coordinates nonlinearly. A simple flow was chosen from which the trajectories are still circular but where the angular velocity is an exponential function of the radius;

$$\Omega(r) = \Omega_0 e^{cr/\Delta s}, \tag{15}$$

or

$$\begin{aligned} u &= -\Omega_0 y e^{cr/\Delta s} \\ v &= +\Omega_0 x e^{cr/\Delta s}. \end{aligned} \tag{16}$$

The nondimensional constant, c , is the percentage change of rotation rate per unit of grid size, Δs . The error (Eq. (12)) is then a function of both c and $\Delta s/r$, the ratio

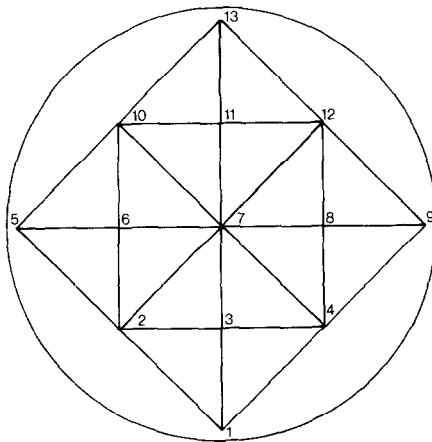


FIG. 5. Initial positions of 13 test particles. The nearshore particles are 2.5 km from the shore boundary, regardless of grid size.

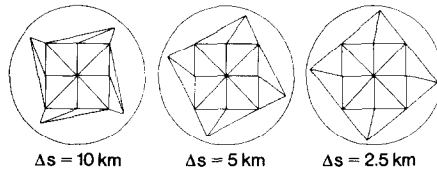


FIG. 6. Test particle positions after one counterclockwise rotation for three grid sizes. The lag of the nearshore particles is caused by the particles following the jagged coastline; thus, the lag increases for coarse resolution grids.

of grid size to the radius. The error, plotted as a function of these two parameters in Fig. 4, is small both for small values of c and for large values of $r/\Delta s$.

To test the effects of shores on the accuracy of the method, particle trajectories are computed in a circular lake. The motion of 13 test particles is calculated; the initial positions of these particles are shown in Fig. 5. In this configuration, particles 1, 5, 9, and 13 start within 2.5 km of the grid boundary for all three grids. In a solid rotation flow using the grid of Fig. 2, these particles could not have exact circular paths without crossing the shore boundary.

Solid rotation for a given grid size is defined as the finite-difference solution

$$\nabla \cdot D^{-1} \nabla \psi = \text{constant}, \tag{17}$$

where D is defined as depth. This definition results in smoother streamfunction contours than would be possible by simply evaluating the solution for solid rotation at the grid points. After one counterclockwise rotation, the 13 particles are as shown

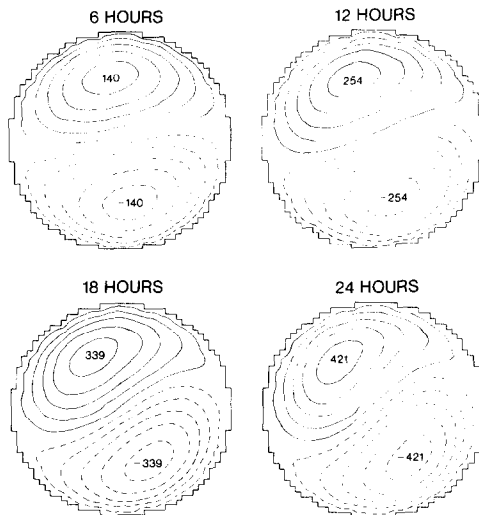


FIG. 7. Current patterns resulting from a 1-day wind stress of 0.1 Nt m^{-2} from the west (left). Solid lines represent counterclockwise flow; dashed lines indicate clockwise flow.

in Fig. 6. Away from the edge of the lake, the solution is nearly exact for all three grid sizes (to about 0.01%). However, the particles near the edge of the lake tend to lag behind, completing 80% of a complete rotation in the 10 km grid and about 95% of a rotation in the 2.5 km grid. This is because the particles follow the shoreline rather than a circular course; hence a large discrepancy occurs with the more irregular shoreline of the coarse resolution grids.

Having evaluated the accuracy of the particle trajectory calculations for solid rotation, the more difficult problem of estimating the error for wind-driven motion will now be discussed. A wind stress pattern typical of a Great Lakes storm was used to drive the model described in [4, 7]. This pattern consists of a 1-day wind stress of 0.1 Nt m^{-2} from the west followed by 4 days with no wind stress. The resulting currents show two gyres, one cyclonic and one anticyclonic, which are initially aligned with the wind. Because of the earth's rotation and the basin topography, these gyres propagate around the basin with a 4-day period. The first 24 h are shown in Fig. 7. This pattern is consistent with the observations of Saylor et al. [3]. Since the numerical solution for wind-driven motion will be used in these calculations, this is a test of the complete method of calculating particle trajectories from currents in a closed basin.

Figure 8 shows the trajectories of the two particles labelled 1 and 2 in Fig. 5, as calculated with grid sizes 10, 5, and 2.5 km. Particle 1, which begins 2.5 km from shore, travels downwind with the current, curving north with the shoreline. The length of the path depends to a great extent on grid size. For the first 2 days, the particle traveled 8 km in the 10-km grid and 16 km in the 2.5-km grid. After 2 days, the motion was negligible for all grid sizes because friction had decreased the current speed in the shallow water. Particle 2 begins further off-shore in the deep water return flow. For the first day, the particle traveled just over 1 km for all grid sizes, but the direction of flow for the 10-km grid differs by 45 degrees from the 5- and 2.5-km grids. For the next 3 days, the particle moves toward the west and northwest as the current direction changes in response to the topographic wave

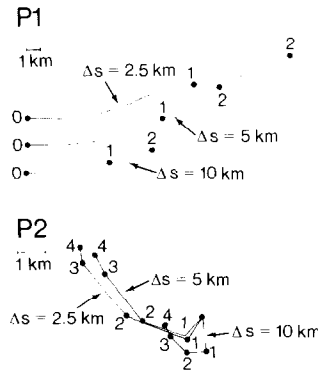


FIG. 8. Particle trajectories for 2 of the 13 test particles. The path length is strongly dependent on grid size. The short path length in the 10-km case is caused mainly by an underestimation of the currents.

motion set up by the west wind. For the higher resolution cases, the particle ends up approximately 4 km from its initial position, but for the 10-km grid it has moved only about 1 km. The reason for this is that the currents in the 10-km grid case decay too fast. In all of these cases the errors are due to the inaccuracies of the current calculations; the errors of the trajectory prediction method discussed here were negligible.

SUMMARY

The purpose of this paper was to test the numerical accuracy of a method that predicts particle trajectories for oil spill cleanup or search and rescue operations. The model uses currents derived from the wind stress to calculate particle trajectories. This paper was motivated by the fact that simple schemes result in particle trajectories that are inaccurate due to time stepping errors which, for the first-order Euler method, cause an outward drift of particles and spatial interpolation errors which can lead to artificial "beaching." The second-order trapezoidal (Crank-Nicholson) method examined here minimizes these problems. It is the simplest second-order time differencing method which uses only two time levels and corrects for particles which beach due to finite-difference errors.

The accuracy of the method was evaluated by computing the trajectories first with a steady solid rotation current pattern and then with time-dependent, wind-driven currents. In the solid rotation case, the technique is very accurate for all grid sizes except for particles near the shore. Because the paths of these particles deviate from pure circles to follow the jagged finite-difference coast, it takes them longer to circumnavigate the lake. The magnitude of this error is about 20% when the radius was five times the grid size (10-km grid) and 5% when the radius was 20 times the grid size (2.5-km grid).

The wind-driven case provides a comparison of the errors in calculating trajectories with the other major source of error for the lake circulation problem—the calculation of the currents from the wind. Offshore, the predicted trajectories for the 2.5- and 5-km grids compare favorably, and since the currents and particle moving schemes are both accurate there, it is reasonable to conclude that these solutions are accurate. Nearshore, the distance that particles move increase as grid size decreases. While both steps of the model cause an underestimation of nearshore speeds, the major errors are due to the current calculation step.

The original oil spill model that was used on the Great Lakes [1] utilized a 14-km grid of Lake Michigan. The solutions presented here for a 10-km grid (Figs. 6 and 8) are clearly not very accurate; the most important source of error is the calculation of currents from the wind stress. Accordingly, the new oil spill model [4] has the capability to use finer grids. Based on Fig. 6, a 5-km grid will be of acceptable accuracy for most areas and will slightly underestimate particle speeds nearshore. However, the resolution of smaller regions or irregular areas may require an even smaller grid size to be accurate.

REFERENCES

1. R. L. PICKETT, "Great Lakes Spill Model," NOAA Tech. Memo. ERL GLERL, 1981, (unpublished).
2. R. L. PICKETT, J. E. CAMPBELL, A. H. CLITES, AND R. M. PARTRIDGE, *J. Great Lakes Res.* **9**, 106 (1983).
3. J. H. SAYLOR, J. C. K. HUANG, AND R. O. REID, *J. Phys. Oceanogr.* **10**, 1814 (1980).
4. D. J. SCHWAB, J. R. BENNETT, AND E. W. LYNN, NOAA Tech. Memo. ERL-GLERL-53, 1984 (unpublished).
5. T. J. SIMONS, G. S. BEAL, K. BEAL, EL SHAARAWI, AND T. S. MURTY, Marine Sciences Directorate, Report No. 37, 1975 (unpublished).
6. G. M. TORGRIMSON, *Proc. Am. Petro. Inst.* **423** (1981).
7. J. R. BENNETT AND J. E. CAMPBELL, *J. Comput. Phys.* **67**, 262, 1986.